Thermal Analysis of V-Corrugated Double-Glazed Dual Purpose Solar Water-Air Heater

Y. Anupam Rao*‡, Aneesh Somwanshi**

*Research Scholar, Department of Mechanical Engineering, MATS University, Raipur, Chhattisgarh, India -493441

** Department of Mechanical Engineering, MATS University, Raipur, Chhattisgarh, India - 493441

(y.anupamrao@gmail.com, aneeshsomwanshi@rediffmail.com)

‡Corresponding Author; Y Anupam Rao, MATS University, Raipur, Chhattisgarh, India -493441

Tel: +919907871234, y.anupamrao@gmail.com

Received: 31.07.2022 Accepted:23.08.2022

Abstract- In the current work, the authors designed and developed a V-Corrugated Double-Glazed Dual-purpose Air-Water Heater (V-DAWH). This device can provide hot air as well as hot water simultaneously. An experimentally verified mathematical model of the suggested design has been created for the weather of Raipur, CG, India (21.2513° N, 81.6295° E). The V-Corrugated Single Glazed Air-Water Heater (V-SAWH) and the Flat Plate Air Water Heater (F-AWH) have been used to compare the performance of the suggested heater (V-DAWH). For a typical winter day, the maximum and minimum air and water temperatures for V-SAWH and F-AWH are 33.2°C and 55.5°C, respectively, at a mass stream rate of 0.01 kg/s. For V-DAWH, air and water are heated to 30.1°C and 51.4 °C, subsequently. The highest air and water temperatures for V-SAWH are 67.2°C and 70.4°C, subsequently. Consequently, as the airflow rate in the upper compartment increases, the degree of heating decreases but the daily efficiency of the heater increases.For V-DAWH With increase in air flow rate from 0.01kg/s to 0.030 kg/s the drop in water temperature and exit air temperature is about 5.4% and 12.3%, respectively. Whereas the efficiency increases by about 3.1%. The maximum daily efficiency for F-AWH and V-SWAH for a day in winter in Raipur, CG, is approximately 83.9% and 66.4%, respectively. V-DWAH operates at a daily efficiency of roughly 64.1%.

Keywords V-Corrugated Double-Glazed Dual-purpose Air-Water Heater (V-DAWH), Flat plate air water heater (F-AWH), V Corrugated single glazed air-water heater(V-SAWH), Mass stream rate.

1. Introduction

The conversion of solar energy to heat, which is employed in solar water and air heaters, is one of the most fundamental harnesses of solar energy. The incident solar energy is straight away converted to heat energy, which is then transferred to either air or water and used for various purposes. The use of flat plate collectors for water heating is fairly popular all over the world.

However, researchers from all around the world are constantly working to improve efficiency of solar energy and impact of Renewable energy [1] even more. Various researchers are working to develop and encourage solar Energy market [2], Furthermore, water heaters are only used for three to four months every year throughout the winter. For the rest of the year, the water heater is not used. Recently, the two technologies of water heating and air heating have been integrated into a single device known as dual-collectors in an attempt to increase the annual consumption of the system. The combination of the two devices, which function as both water and air warmers, boosts the overall annual use of solar energy. It may provide hot water and hot air as needed, or it can be used individually as a water and air heater. Some of the works on dual-purpose solar air and water heater has been reported in the past [3-9].Some of the recent works related to the development of air/water heaters included in the works done by [10-13], to increase the performance of heater they suggested to add aluminium chip, paraffin wax, nano-SiC, Fluorine doped Tin Oxide(FTO) , Mixed Asphalt and Aluminum(III)Oxide. Another study to improve performance of heat collection is done by[14] in which simulation model of liquid solar sytem has been investigated. Recently [15] experimentally studied a dual-purpose solar thermal collector for heat as well as cold collection.One more study [16] shows the feasibility of multistage solar still in devloping countries.Study on Reducing Corrosion effects to enhance efficiency is done by[17]

A dual-function collection-cum storage kind of air-water heater (DCS-AWH), which combines a water heater and an

air heater into a single device that can heat both air and water, was recently proposed by[18]. Unlike prior dual-collector designs that have been proposed. The proposed design is simple in construction: it consists of two insulated rectangular compartments and a common absorber plate separates them. The upper single-glazed chambers are used as an air heater whereas the lower chamber contains water that gets heated due to heat transfer by the absorber plate. In the current work, the previously proposed design has been modified, in place of a single glass cover, the new design includes a double glass cover to reduce the overall top loss coefficient. Moreover, to increase the collection area, a flat absorber plate has been superseded by a V-grooved corrugated absorber plate. Unlike the previous proposed designs of dual function air-water heater, the proposed design is simple in construction. The dual function heater delivers hot air as well as hot water simultaneously. The single device functions in dual mode increases the overall annual usage hence it is more cost effective. The introduction of the V corrugated absorber plate enhances the rate of heat transfer to water as well as air, it improves the overall performance of the device further more than the previous proposed designs.

The use of V- corrugated plate instead of a flat absorber plate has been used in past in air and water heaters to boost the coefficient of heat transfer and overall collection area[19-26]. To enhance the performance of solar water heater the absorber plate has been modified by adding the aluminium foam by [27]. They found the increase in thermal efficiency of about 10.21% by introducing the modified absorber plate.

The objective of the work is to design and develop a double-glazed V corrugated absorber plate dual purpose air-water heater that can deliver hot air as well as hot water. The extended objective is to present the mathematical model of the proposed design and to validate the proposed model by conducting experiment in the weather of Raipur, CG, India (21.2513° N, 81.6295° E). Furthermore, the authors performed numerical computations to compare the daily performance of the proposed V-Corrugated Double-Glazed Dual function air-water heater (V-DAWH) with that of single glazed dual function air/water heater (V-SAWH) and Flat plate dual function air/water heater (F-AWH) for the weather of Raipur, CG, India (Fig.1).

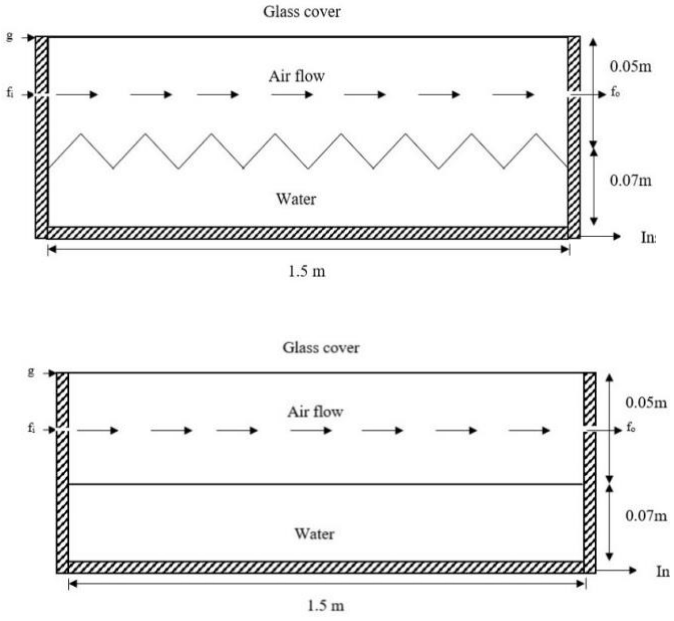

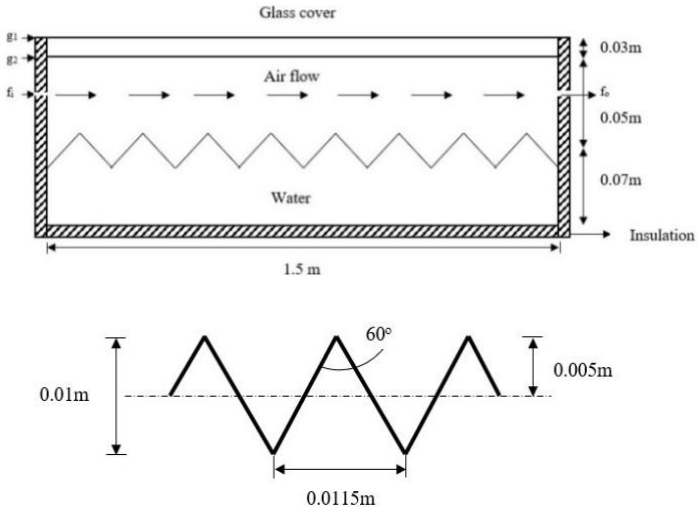

Fig.1. Schematic diagram of V-DAWH, V-SAWH & F-AWH and part of v-corrugated plate

The upper chamber mass stream rate of moving air will have an impact on the heater's overall performance. Numerical computation has been done to examine the impact of mass stream rate. The expanded goal of the current study is to determine the level of water and air heating as well as the daily efficiency of the suggested device.

2. Mathematical Model and Experimental Setup

The assumptions that have been considered while performing energy analysis are as follows-

1. The absorber plate is reckoned as a plane surface for calculating incident solar radiation because the depth of the corrugation is less.
2. The temperature only varies in the path of the air and water flow.
3. The framework is in a quasi-steady state condition.
4. The flow rate of air is assumed as constant.
5. Since it is assumed that the collector area will be larger than its thickness, the losses from the sides are ignored.

2.1 V Corrugated Double-Glazed Dual-Purpose Air/Water Heater

The equations for the energy balances of the top and bottom glass covers, air flow, absorber plate, water, and basin are as follows:

For Top glass cover (g_1)

$$U_t(T_{g1}-T_{amb}) = h_{cag1}(T_a-T_{g1}) + h_{rg2g1}(T_{g2}-T_{g1}) + \alpha_g I \quad (1)$$

h_{camb}, h_{ramb} and h_{rg2g1} will be given by [28]

$$U_t = h_{camb} + h_{ramb} \quad (2)$$

$$h_{camb} = 2.8 + 3v_a \quad (3)$$

$$h_{ramb} = \frac{\varepsilon_g \sigma[(T_{g1}+273)^4 - (T_{amb}+267)^4]}{T_{g1} - T_{amb}} \quad (4)$$

$$h_{rg2g1} = \frac{\varepsilon_{eff} \sigma[(T_{g2}+273)^4 - (T_{g1}+273)^4]}{T_{g2} - T_{g1}} \quad (5)$$

h_{cag1} is given by [29]

$$h_{cag1} = 1.25(\Delta T_g)^{1.25} \quad (6)$$

Solving Eqn. 1 and 2 we have,

$$T_{g1} = K_1 T_{g2} + K_2 \quad (7)$$

Constants K_1 and K_2 are given by,

$$K_1 = \frac{h_{g2g1}}{U_t + h_{g2g1}}$$

$$K_2 = \frac{U_t T_{amb} + \alpha_g I}{U_t + h_{g2g1}}$$

For Lower glass cover (g_2)

$$I\alpha_g \tau_g + h_{rpg2}(T_p - T_{g2}) + h_{cfg2}(T_f - T_{g2}) = h_{rg2g1}(T_{g2} - T_{g1}) + h_{cag2}(T_{g2} - T_a) \quad (8)$$

$$h_{cag1} = h_{cag2} \quad (9)$$

The relationship between the fluid and bottom glass cover's convective heat transfer coefficient is given by [30-32].

Re 2800 is recommended for laminar flow

$$Nu = 4.4 + \frac{0.0039(0.7\,\mathrm{Re}\,D_h / L)^{1.66}}{1 + 0.0114(0.7\,\mathrm{Re}\,D_h / L)^{1.12}} \quad (10)$$

Re>2800 For turbulent flow

$$Nu = 0.0158\,\mathrm{Re}^{0.8}(1 + \frac{D_h}{L})^{0.7} \quad (11)$$

In Eq. 10 and 11, Re Reynold's number, D_h and L hydraulic diameter of duct and length of collector, respectively. They are given by,

$$\mathrm{Re} = \frac{\rho_f v_f D_h}{\mu_f} \quad (12)$$

$$D_h = \frac{4WH}{2(W+H)} \quad (13)$$

In Eq.12 and 13, ρ_f, v_f, μ_f are density, velocity and dynamic viscosity of fluid(air) in the upper compartment. The height and width of upper compartment is indicated by H and W. Form Eq. 7,

$$h_{cfg2} = \frac{k_f Nu}{D_h} \quad (14)$$

The heat transfer coefficient between corrugated absorber plate and a flowing fluid is given by [33],

$$h_{cpf} = (\frac{k_f Nu}{D'_h}) \frac{1}{\sin(\theta/2)} \quad (15)$$

The corrugated angle θ will give the approximate hydraulic diameter of the duct

$$D'_h = H_{\min} + b$$

Here $H_{\min}$ is the minimum height of the air channel and b is Groove's half height, and θ is groove angle.

The fluid (air) properties between temperatures (5°C-100°C) will be given by,

$$\rho_f = 10^{-5} T_f^2 - 0.0045 T_f + 1.2908$$

$$K_f = -5\times10^{-8} T_f^2 + 8\times10^{-5} T_f + 0.0241$$

$$\mu_f = (-4\times10^{-6} T_f^2 + 0.0049 T_f + 1.7231)10^{-5}$$

From Eq.7 and 8, we have

$$T_{g2} = K_3 T_p + K_4 T_f + K_5 \quad (16)$$

Here constants K_3, K_4 and K_5 will be given by,

$$K_3 = \frac{h_{rpg2}}{U_t K_1 + h_{rpg2} + h_{cfg2}}$$

$$K_4 = \frac{h_{cfg2}}{U_t K_1 + h_{rpg2} + h_{cfg2}}$$

$$K_5 = \frac{\alpha_g I(\tau_g + 1) - U_t K_2 + U_t T_{amb}}{U_t K_1 + h_{rpg2} + h_{cfg2}}$$

For the flow of fluid (air) between the absorber plate and the lower glass cover (g_2)

The energy balance of flowing air for length '*dx*' is given by

$$\dot{m}_f c_a \frac{dT_f}{dx} dx = h_{cpf}(T_p - T_f) L_2 dx + h_{cfg2}(T_{g2} - T_f) L_2 dx \quad (17)$$

Eq. 17 can be given by,

$$T_f(L_1) = A T_p + B \quad (18)$$

Here,

$$A = \frac{B_1}{A_1}(1 - \exp(-A_1 L_1) \quad (19)$$

$$B = \frac{B_2}{A_1}(1 - \exp(-A_1 L_1) + T_{f0} \exp(-A_1 L_1) \quad (20)$$

$$A_1 = \frac{h_{cpf} L_2 + h_{cfg2} L_2 - h_{cfg2} K_4 L_2}{\dot{m}_f c_a}$$

$$B_1 = \frac{h_{cpf} L_2 + h_{cfg2} K_3 L_2}{\dot{m}_f c_a}$$

$$B_2 = \frac{h_{cfg2} K_5 L_2}{\dot{m}_f c_a}$$

The average fluid temperature will be given by,

$$\bar{T}_f = \frac{1}{x}\int_0^x T_f(x)dx \tag{21}$$

For $x = l_1$ the average fluid temperature will be given by,

$$\bar{T}_f = X_1 T_p + X_2 \tag{22}$$

Here constants X_1, X_2 are given by,

$$X_1 = \frac{B_1}{A_1}[1-\frac{(1-\exp(-A_1L_1)}{A_1L_1}]$$

$$X_2 = \frac{B_2}{A_1}[1-\frac{(1-\exp(-A_1L_1)}{A_1L_1}]+T_{f0}\frac{(1-\exp(-A_1L_1)}{A_1L_1}$$

T_{f0} Is the temperature of the fluid at the inlet which is equal to ambient temperature T_{amb}

For Absorber Plate

$$\alpha_p\tau_g^2 I = h_{cpf}(T_p - T_f) + h_{rpg2}(T_p - T_{g2}) + h_{cpw}(T_p - T_w) \tag{23}$$

In Eq. 15, h_{cpw} is convective heat transfer coefficient due to natural convection between the inclined plate and water and is determined by relation [34],

$$Nu = 0.56(Gr_e \,\mathrm{Pr}_e \cos\theta)^{1/4}$$

$$10^5 < Gr_e \,\mathrm{Pr}_e \cos\theta < 10^{11} \tag{24}$$

θ is the angle formed by the absorber surface and the vertical, The values of Gr_e and Pr_e are calculated at a temperature given by $T_e = T_p - 0.25(T_p - T_w)$ volumetric heat transfer coefficient β will be determined at temperature $T'_e = T_w - 0.5(T_w - T_{amb})$ Gr_e and Pr_e will be given by,

$$Gr_e = \frac{g\beta\Delta T L_c^3}{\upsilon^2} \tag{25}$$

$$\mathrm{Pr}_e = \frac{\upsilon}{\alpha} = \frac{c_p\mu}{K} \tag{26}$$

L_c is the characteristic length of the absorber plate, υ and α are kinematic viscosity and thermal diffusivity, subsequently.

For the temperature range between 5°C to 100°C kinematic viscosity, thermal conductivity and Prandtl number will be given by,

$$\upsilon = (3\times10^{-8}T_e^4 - 8\times10^{-6}T_e^3 + 0.009T_e^2 - 0.0516T_e + 1.7481)10^{-6}$$

$$K = 1\times10^{-5}T_e^2 + 0.0022T_e + 0.5595$$

$$\mathrm{Pr} = -2\times10^{-5}T_e^3 + 0.0042T_e^2 - 0.3461T_e + 12.566$$

From Eqs. 16, 22 and 23 we have,

$$T_p = K_6 T_w + K_7 \tag{27}$$

Here constants K_6 and K_7 are given by,

$$K_6 = \frac{h_{cpw}}{h_{cpf} - h_{cpf}X_1 + h_{rpg2} - h_{rpg2}K_3 - h_{rpg2}K_4X_1 + h_{cpw}}$$

$$K_7 = \frac{\alpha_p\tau_g^2 I + h_{cpf}X_2 + h_{rpg2}K_4X_2 + h_{rpg2}K_5}{h_{cpf} - h_{cpf}X_1 + h_{rpg2} - h_{rpg2}K_3 - h_{rpg2}K_4X_1 + h_{cpw}}$$

For Basin,

$$h_{cwb}A_b(T_w - T_b) = U_bA_b(T_b - T_{amb}) \tag{28}$$

U_b in the above equation is the loss coefficient from bottom

$$U_b = \frac{K_b}{t_b} \tag{29}$$

From Eq. 28 we have

$$T_b = K_8T_w + K_9 \tag{30}$$

Values of constants K_7 K_8 are given by,

$$K_8 = \frac{h_{cwb}}{U_b + h_{cwb}}$$

$$K_9 = \frac{U_bT_{amb}}{U_b + h_{cwb}}$$

For water in the basin

$$M_wc_w\frac{dT_w}{dt} = h_{cpw}A_p(T_p - T_w) - h_{cwb}A_b(T_w - T_b) \tag{31}$$

From Eq. 27, 30 and 31, we have

$$T_w(t) = \frac{K_{11}}{K_{10}}[1-\exp(-K_{10}t)] + T_{w0}\exp(-K_{10}t) \tag{32}$$

T_{w0} is the initial water temperature, the constants K_{10} and K_{11} will be given by,

$$K_{10} = \frac{h_{cpw}A_p + h_{cwb}A_b - h_{cpw}A_pK_6 - h_{cwb}K_8A_b}{M_wc_w}$$

$$K_{11} = \frac{h_{cpw}A_pK_7 + h_{cwb}A_bK_9}{M_wc_w}$$

Eq.32 can be solved to give water temperature concerning time, the temperature of the absorber plate will be determined by Eq. 27and the outlet temperature of the fluid (air) will be determined by Eq. 18.

2.2 V corrugated plate single glazed air-water heater

The Energy balances of the glass cover, fluid flowing (air flowing), water and basin, absorber plate are given below

Glass cover

$$U_t(T_g - T_{amb}) = h_{cpf}(T_f - T_g) + h_{rpg}(T_p - T_g) + \alpha_g I \tag{33}$$

From Eq.1,

$$T_g = K_{1x}T_f + K_{2x}T_p + K_{3x} \quad (34)$$

Constants, K_{1x}, K_{2x} and K_{3x} will be given by,

$$K_{1x} = \frac{h_{cpf}}{U_t + h_{cpf} + h_{rpg}}$$

$$K_{2x} = \frac{h_{rpg}}{U_t + h_{cpf} + h_{rpg}}$$

$$K_{3x} = \frac{\alpha_g I + U_t T_{amb}}{U_t + h_{cpf} + h_{rpg}}$$

For Fluid Flowing

$$\dot{m}_f c_a \frac{dT_f}{dx} dx = h_{cgf}(T_g - T_f)L_2 dx + h_{cpf}(T_p - T_f)L_2 dx \quad (35)$$

From Eq. 34 and 35,

$$\frac{dT_f}{dx} + A_{1x}T_f = B_{1x}T_p + B_{2x} \quad (36)$$

$$A_{1x} = \frac{h_{cpf}L_2 + h_{cfg}L_2 - h_{cfg}K_{1x}L_2}{\dot{m}_f c_a}$$

$$B_{1x} = \frac{h_{cfg}K_2 L_2 + h_{cpf}L_2}{\dot{m}_f c_a}$$

$$B_{2x} = \frac{h_{cfg}K_3 L_2}{\dot{m}_f c_a}$$

From Eq.13, the fluid temperature $x = L_1$ will be given by,

$$T_{fl} = A_x T_p + B_x \quad (37)$$

The average fluid temperature will be given by,

$$\overline{T}_f = X_{1x}T_p + X_{2x} \quad (38)$$

Values of constants A_x, B_x X_{1x} and X_{2x} will be given by,

$$A_x = \frac{B_{1x}}{A_{1x}}(1 - \exp(-A_1 L_1)$$

$$B_x = \frac{B_{2x}}{A_{1x}}(1 - \exp(-A_{1x}L_1) + T_{f0}\exp(-A_{1x}L_1)$$

$$X_{1x} = \frac{B_{1x}}{A_{1x}}[1 - \frac{(1 - \exp(-A_{1x}L_1)}{A_{1x}L_1}]$$

$$X_{2x} = \frac{B_{2x}}{A_{1x}}[1 - \frac{(1 - \exp(-A_{1x}L_1)}{A_{1x}L_1}] + T_{f0}\frac{(1 - \exp(-A_{1x}L_1)}{A_{1x}L_1}$$

For absorber plate

$$(\alpha\tau)I = h_{cpf}(T_p - T_f) + h_{rpg}(T_p - T_g) + h_{cpw}(T_p - T_w) \quad (39)$$

From Eq. 34, 38 and 39, we have

$$T_p = K_{4x}T_w + K_{5x} \quad (40)$$

$$K_{4x} = \frac{h_{cpw}}{h_{cpf} - h_{cpf}X_{1x} + h_{rpg} - h_{rpg}K_{2x} - h_{rpg}K_{1x}X_{1x} + h_{cpw}}$$

$$K_{5x} = \frac{(\alpha\tau)I + h_{cpf}X_2 + h_{rpg}K_{1x}X_2 + h_{rpg}K_{3x}}{h_{cpf} - h_{cpf}X_{1x} + h_{rpg} - h_{rpg}K_{2x} - h_{rpg}K_{1x}X_{1x} + h_{cpw}}$$

For basin

$$h_{cwb}A_b(T_w - T_b) = U_b A_b(T_b - T_{amb}) \quad (41)$$

From Eq. 41 we have,

$$T_b = K_{6x}T_w + K_{7x} \quad (42)$$

Here constants K_{6x} and K_{7x} will be given by,

$$K_{6x} = \frac{h_{cwb}}{U_b + h_{cwb}}$$

$$K_{7x} = \frac{U_b T_{amb}}{U_b + h_{cwb}}$$

For water in the basin

$$M_w c_w \frac{dT_w}{dt} = h_{cpw}A_p(T_p - T_w) - h_{cwb}A_b(T_w - T_b) \quad (43)$$

From Eq. 40, 42 and 43, we have

$$T_w(t) = \frac{K_{9x}}{K_{8x}}[1 - \exp(-K_{8x}t)] + T_{w0}\exp(-K_{8x}t) \quad (44)$$

T_{w0} is the initial water temperature, the constants K_{10} and K_{11} will be given by,

$$K_{8x} = \frac{h_{cpw}A_p + h_{cwb}A_b - h_{cpw}A_p K_{4x} - h_{cwb}K_{6x}A_b}{M_w c_w}$$

$$K_{9x} = \frac{h_{cpw}A_p K_{5x} + h_{cwb}A_b K_{7x}}{M_w c_w}$$

Eq.44can be solved to give water temperature concerning time, temperature of air exit will be found out by Eq. 37.

2.3 Single Glazed Flat Plate Air-water Heater

For flat plate single glazed air/water heater all the equations are the same as for single glazed V corrugated plate air/water heater only the convective coefficient between the plate and air (h_{cpf})and plate and water (h_{cpw})will change accordingly.

$$h_{cpf} = \frac{NuK}{D_h} \quad (45)$$

Nusselt number will be given by [35],

$$Nu = \frac{0.01344\,\mathrm{Re}^{0.75}}{1 - 1.586\,\mathrm{Re}^{-0.125}}$$

In Eq.45 the significance of the Nusselt number is the same as given by Eq.10,11. D_h is given by Eq. 13.

The convective heat transfer coefficient between plate and water will be given by

$$Nu = 0.54(Gr\,\mathrm{Pr})^{1/4} \quad (46)$$

$$h_{cpw} = \frac{K}{X_L}0.54(Gr\,\mathrm{Pr})^{1/4} \quad (47)$$

In Eq. 47, the characteristic length X_L will be given by,

$$X_L = A_p / P \quad (48)$$

2.4 Experimental Setup Design of the Proposed Heater

The design of the proposed heater is a modification of the earlier design of the dual-purpose solar air-water heater (DSC-AWH) proposed by [18].It is made up of two insulated compartments partitioned by a common absorber plate. The upper section can be utilized for air heating, while the lower compartment holds water and serves as a water heater. To enhance the rate of heat transfer and collection area, the flat absorber plate proposed previously has been replaced by a V-shaped corrugated absorber plate in the current work. The plate is painted black to absorb solar radiation, and the corrugation depth is kept to a minimum (0.01m). The pitch is approximately0.0115m, and the angle is 60°C [36]. To minimize the top loss from the glass cover, it has been replaced by a double glass cover (0.003m thick). The heater was insulated from bottom & sides by glass wool of 0.05m thickness. The proposed device can function in dual mode as well as be used in single mode. An electrical water heating element is fixed in the lower compartment which can be used to heat water during bad weather whenever required. Fig. 2 depicts the proposed design's schematic. Table 1 lists the proposed heater's other design parameters.

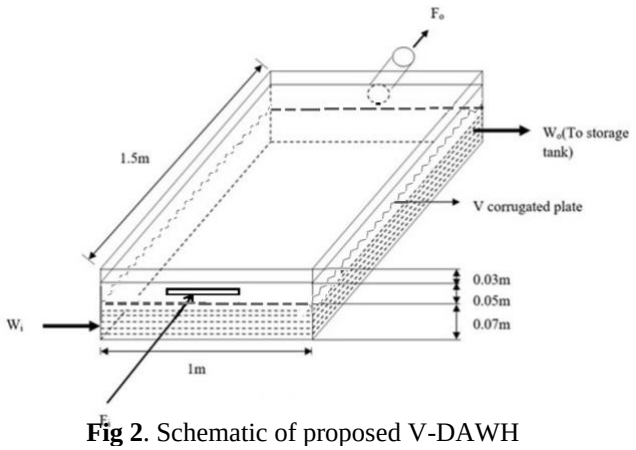

Fig 2. Schematic of proposed V-DAWH

Table 1 Parameters of Design of planned V –DAWH

Size	Length	160cm
	Breadth	110cm
	Height	20cm
Material	M S plate	0.3cm
Insulating pad	Glass wool	0.4cm
Transparent covers	Glass	0.4cm (thickness), 1.5m^2(area)
Absorber Plate	MS Plate	Painted Black
	V-Grooved	
Collector area		1.5m^2
Frame	Wooden	
Dimensions of Air Channel	Length	150cm
	Breadth	100cm
	Height	5cm
	Air duct diameter	15cm
Dimensions of Water Channel	Length	150cm
	Breadth	100cm
	Height	7cm
Water tank Capacity		105L
V- groove	Depth	1cm
	Pitch	1.15cm
	Angle	60º

2.5 Validation of Mathematical Model

A test trial is done at Raipur, CG, India in October (16/10/2021) to validate the analytical results. Raipur is a city in the state of Chhattisgarh, situated in central part of India. District Raipur Extends from latitude 21° 23″ to longitude 81° 65″. Over the course of the year, the temperature typically varies from 57°F to 106°F and is rarely below 51°F or above 112°F.The monthly maximum and minimum temperature for various months during a year is shown in Fig. 3[37]

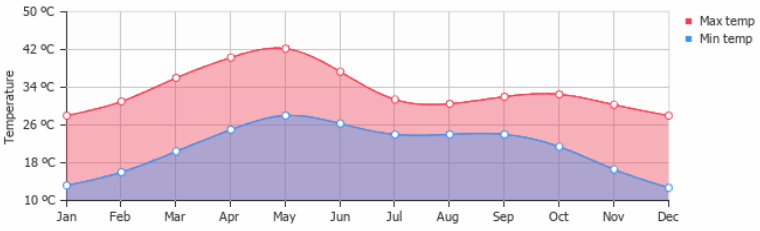

Fig 3. Monthly maximum and minimum temperature of Raipur, Chhattisgarh [37]

The heater was replenished with fresh water in the early morning for about one hour (7.00AM) before taking observations. An initial value of the temperature of glass covers, corrugated plates and water has been recorded as 25.4ºC, 23.5ºC, 27.5ºC and 22.5ºC, respectively. Primal temperature of the fluid (air) to be heated flowing in the upper compartment is equal to the ambient temperature of the air. Fig. 2 and 4 show a delineative diagram of the experimental setup as well as actual photograph of the setup. RTDs connected at various points measure the temperature of the glass cover, plate, and water. The average temperature is used in subsequent calculations.

A pyranometer placed over the glass cover measures the solar radiation that strikes it. The entire setup is placed at an angle equal to the latitude of the location. So that maximum solar radiation can be achieved all time during the year. Water and exit air temperatures are recorded at one-hour intervals until sunset in the evening, up to 6.00 PM. A hot wire anemometer was used to measure the velocity of the air coming from the outlet dust in order to calculate the mass stream rate of air flowing in the upper compartment.

Fig.4 Photograph of Experimental Setup of V-DAWH

The mass stream rate as determined during the experiment was 0.0297kg/s. The solar radiation and ambient air temperature during the experiment are shown in Fig.5. The makes and accuracy of various instruments which were utilized in setup to perform experiment is shown in Table 2.

Table 2 Instruments utilized at the time of Experiment

Device	Range	Precision	% Uncertainty
Constantan K-type Temperature Sensor	0°C to 150°C	±0.2°C	2% to 0.4% (10°C to 50°C)
Platinum RTD-Temperature Sensor	-50°C to 199.9°C	±0.1°C	1% to 0.2% (10°C to 50°C)
Digital Lutron AM-420 Anemometer	0.0m/s to 45.0m/s	±0.1m/s	5% (2m/s)
Kipps & Zenon Pyranometer	0W/m^2 to 1500W/m^2	73µV/W/m^2 (Sensitivity)	10%
Chronometer	-	±0.01s	-

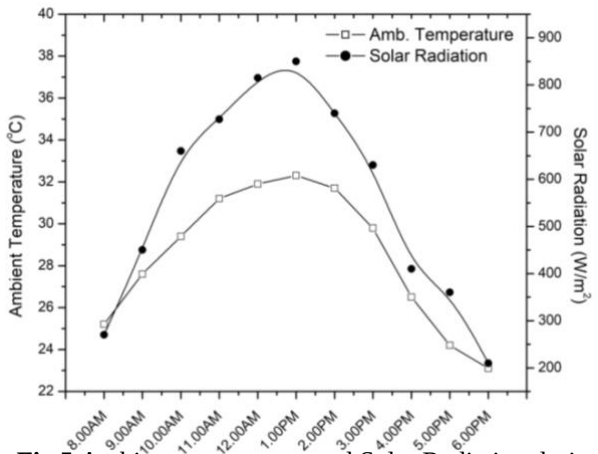

Fig.5 Ambient temperature and Solar Radiation during

The temperature of water and exit air is numerically computed by the proposed mathematical model and it is compared with experimental observations and shown in Figs.6 and 7. It is observed that the recorded values are contiguous to theoretical values. The small variations in the values are due to the average values of coefficients considered for computations. To determine the closeness of recorded and theoretical values, we have determined the coefficient of correlations (r) and root mean of percentage deviation (e) which is given by,

$$e = \sqrt{\frac{\sum (e_i)^2}{n}}$$

$$e_i = [\frac{X_{pre(i)} - X_{expt(i)}}{X_{pre(i)}}] \times 100$$

$$r = \frac{N_x \sum X_{th} X_{ex} - (\sum X_{th})(\sum X_{ex})}{\sqrt{N_x \sum X_{ex}^2 - (\sum X_{ex})^2} \sqrt{N_x \sum X_{th}^2 - (\sum X_{th})^2}}$$

Here N_x is no of readings.

The experimental values are reasonably close to theoretical values as shown in Fig.6& Fig 7. The values of the RMS of percentage deviation (e) and correlation coefficient (r) are between 8.01 to 10.58 and 0.9913to 0.9869, respectively.

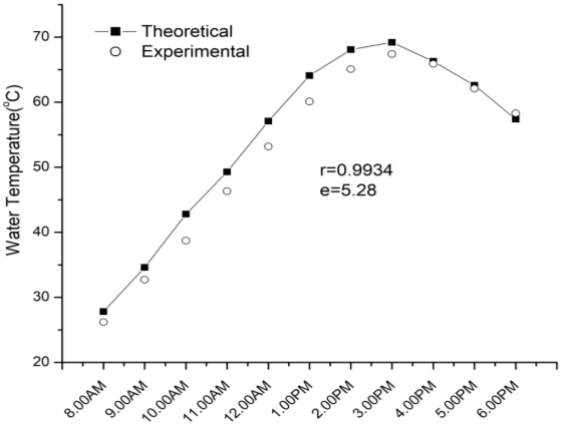

Fig.6 Theoretical and Experimental Water Temperature

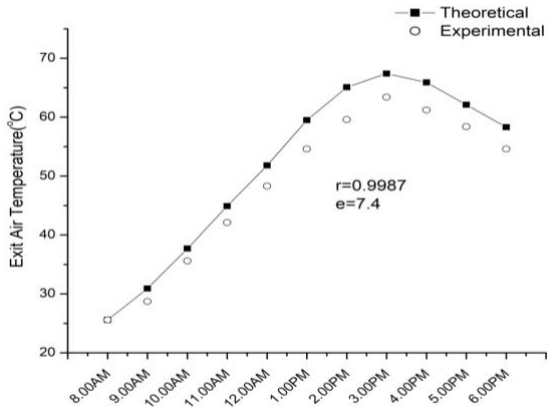

Fig.7 Theoretical and Experimental Air Temperature

3 . Results and Discussions

3.1. Performance of proposed heater by varying mass stream rate of air in upper compartment

The device's total performance will depend on how much air is moving through the upper compartment at any one time. Numerical calculations have been made to determine the air and water temperatures as functions of the mass stream rate of air for the proposed heater in order to examine the effect of the air flow rate. The device's total performance will depend on how much air is moving through the upper compartment at any one time. Numerical calculations have been made to determine the air and water temperatures as functions of the mass stream rate of air for the proposed heater in order to examine the effect of the air flow rate. For computations an hourly average of ambient temperature and solar radiations were considered for a typical day in the weather of Raipur, CG, India Fig.8. The initial glass temperature, plate temperature, water temperature was assumed to be nearly equal to ambient temperature. The rest of the significant parameters are the same as discussed earlier. Other significant parameters that are used for computations are shown in Table 3.

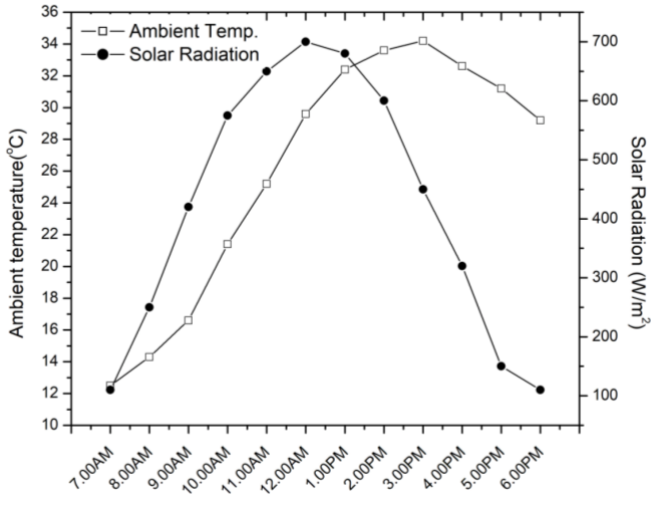

Fig.8 Ambient Air Temperature and Solar Radiation for a typical Day(21/10/2021) in winter for Weather of Raipur (CG, India).

Table 3 Relevant Parameters used for Numerical Computations

M_w	105Kg
L_1	1.5m
εeff	0.85
τ_g	0.9
c_w	4200 J/kgK
σ	$5.67X10^{-8}W/m^2K^4$
v_a	1m/s
t_b	0.05m
c_a	1005J/KgK
α_g	0.9
k_b	0.004W/mK
ατ	0.85
ε_g	0.88
h_{cwb}	$108W/m^2K$
A_g	$1.5m^2$
α_p	0.9
A_b	$1.5m^2$

Figs.9 and 10 show that the increase in water and air temperature is less as the mass stream rate of air increases in the upper compartment. This is because there is less time for the heated plate to come into contact with the air at a higher velocity, which slows down the rate at which the air is heated. As a result, the temperature of the water stored in the lower compartment also drops as the mass stream rate of air increases. The temperature of the water drops by roughly 5.4 percent while the temperature of the exit air drops by around 12.3 percent as the mass stream rate of air increases from 0.010 to 0.030kg/s.

Fig.9 Mass Stream Rate of Air Effect on Water Temperature

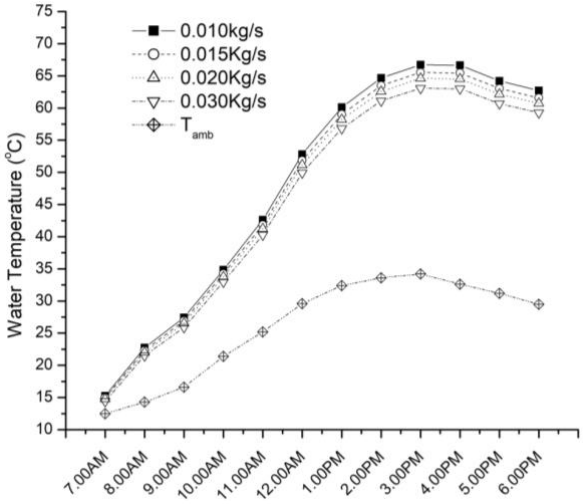

Fig.10 Mass Stream Rate of Air Effect on Exit Air Temperature

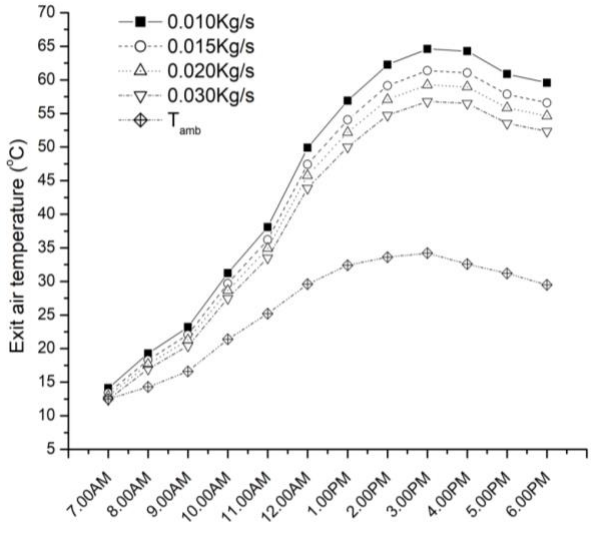

3.2. Performance of the Proposed Heater

The hourly storage temperatures of the water and exit air for a day in the winter month (21/10/2021) have been calculated numerically in order to assess the effectiveness of the suggested heater. The proposed heater's performance is contrasted with that of the V-corrugated single glazed air/water heater (VSAWH) and the flat plate air water heater (FPAWH). All designs and dimensions are held constant throughout the comparison; only the flat plate is taken into account when evaluating the FPAWH. Air is thought to move at a mass stream rate of 0.010 kg/s.

The degree of heating is another parameter that defines the performance of the heating device. The amount of heating in air is determined by the difference between the temperature at exit and the temperature at inlet $(T_{fe} - T_{fi})$, and the amount of heating in water is determined by the difference between the temperature at storage and the temperature at intake $(T_w - T_{w0})$. The degree of cooling of air and water has been determined for a day in winter for which the ambient temperature varies between 12.5°C to 34.2°C whereas the maximum solar radiation received is 700W/m^2.

It is seen from Figs 11&12, that the maximum water temperature is about 70.4°C for V corrugated single glazed air/water heater. The maximum water temperature for V corrugated double glazed air/water heater is about 66.3°C whereas for flat plate air/water heater maximum water temperature attained is about 56.2°C. Moreover, the maximum water temperature reaches around 3.00PM. Similarly, the maximum temperature of exit air is 67.2°C for V corrugated single glazed air/water heater and it is about 64.2°C for V corrugated double glazed air/water heater. Whereas the flat plate air/water heater has a temperature of 51.4°C.

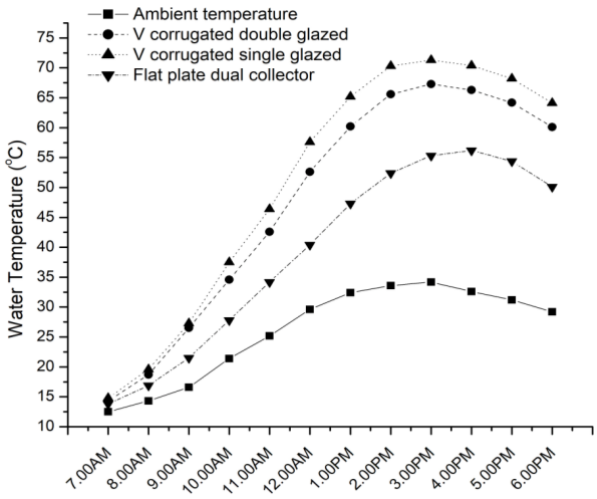

Fig. 11 Temperature of Water for a Typical Day(21/10/2021) in Winter for Raipur Weather Temperature

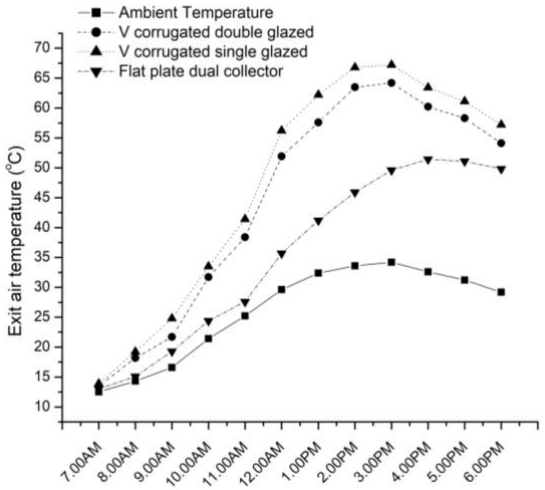

Fig. 12 Outlet Air Temperature for a Typical Day (21/10/2021) in Winter for Raipur Weather

It has been shown in Figs.13 & 14,that air is heated more efficiently with a V-corrugated plate than with a flat plate heater due to an increase in the heat transfer coefficient. In contrast to a V-corrugated double-glazed air/water heater, a single-glazed air/water heater has a higher maximum temperature for both air and water. Although the top loss coefficient is reduced with a double glass cover, the transmittance-absorptance product decreases overall.

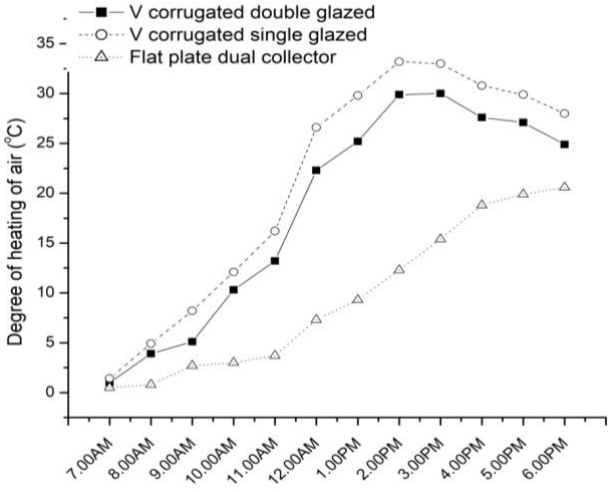

Fig. 13 Degree of Heating of Air for a Typical Day(21/10/2021) in Winter for weather of Raipur, CG, India

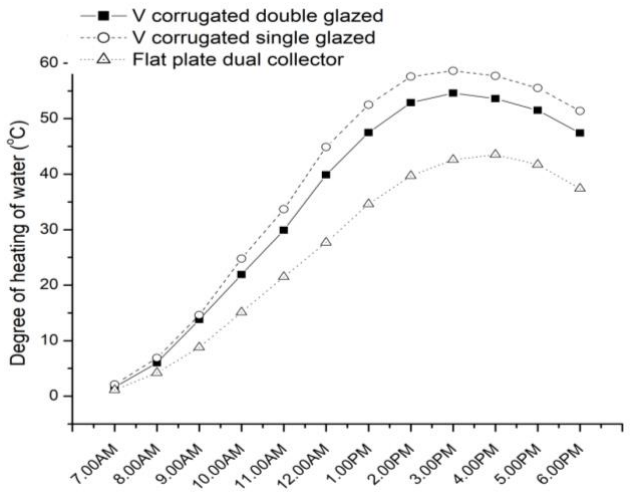

Fig. 14 Degree of Heating of Water for a Typical Day(21/10/2021) in Winter for weather of Raipur, CG, India

3.3. Daily Efficiency

The heater's overall efficiency will be represented by,

$$\eta = \frac{q_{ua} + q_{uw}}{q_r} \tag{49}$$

q_{ua} and q_{uw} are the total useful heat extracted from air and water respectively, it is given by

$$q_{ua} = \sum \dot{m}_f c_a (T_{fl} - T_{amb}).t \tag{50}$$

$$q_{uw} = M_w c_w (T_{fw} - T_{wi}) \tag{51}$$

$$\eta = \frac{\sum \dot{m}_f c_a (T_{fl} - T_{amb}).t + M_w c_w (T_{wf} - T_{w1})}{\sum I A_p t} \tag{52}$$

T_{wi} and T_{wo} are initial and final water temperature, t is the total time to reach from T_{wi} to T_{wo}

The efficiency of the heater is influenced by the mass stream rate of the air moving in the upper compartment. The suggested V corrugated double glazed air-water heater's total daily efficiency has been calculated by adjusting the mass stream rate, as illustrated in Fig.15, to analyse the impact of mass stream rate. It can be shown that efficiency rises when the air mass stream rate in the top compartment increases, despite a drop in water and exit air temperatures. Although the temperature of the air and water exiting the system is lowered as a result of less time spent in contact with the heated plate as the mass stream rate increases, overall system efficiency rises. It can be seen that the heater's efficiency ranges from 64.1% at a mass stream rate of 0.01 kg/s to 66.1% at a mass stream rate of 0.03 kg/s. As a result, the daily efficiency is raised by roughly 3.1%. Additionally, it is shown that efficiency nearly remains unchanged above a mass stream rate of 0.03 kg/s.

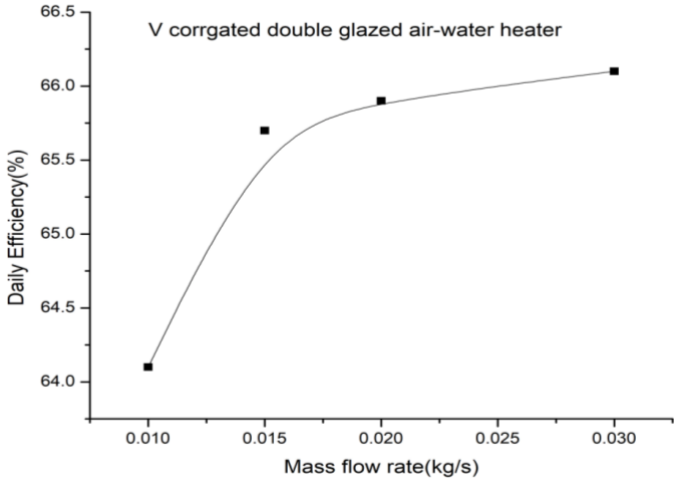

Fig. 15 Effect of Mass Stream Rate on Efficiency

Fig.16 compares the proposed double-glazed heater's daily efficiency to that of a single-glazed and flat-plate air-water heater. The flat plate air-water heater has an efficiency of up to 83.9%, while single- and double-glazed air-water heaters have efficiency of 64.1% and 66.4%, respectively.The flat plate air water heater has the highest efficiency when compared to earlier works on dual function air water heaters (Fig. 17), while the efficiency of the proposed V-DAWH and V-SAWH is lower when compared to work by [3] and almost same as [4]. However, when the temperature requirement of water and air is high, the proposed V-SAWH can deliver at a relatively hot temperature.

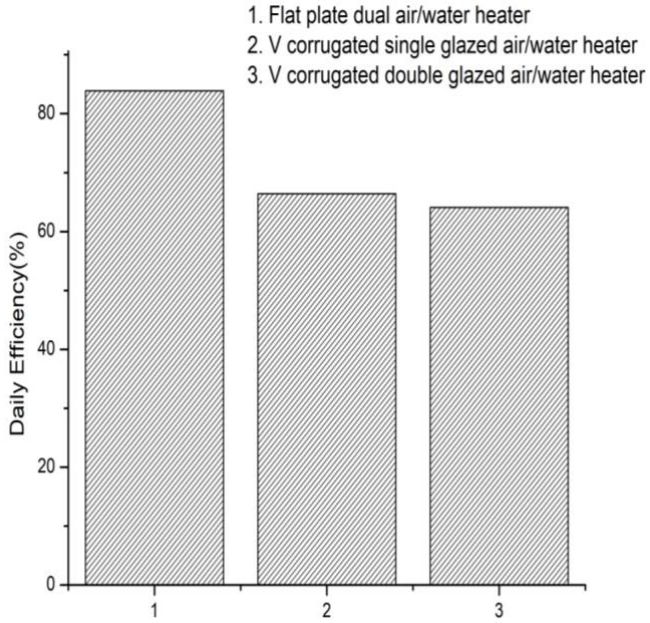

Fig.16 Efficiency of V-Corrugated Single Glazed, V-Corrugated Double Glazed and Flat Plate Air/Water Heater

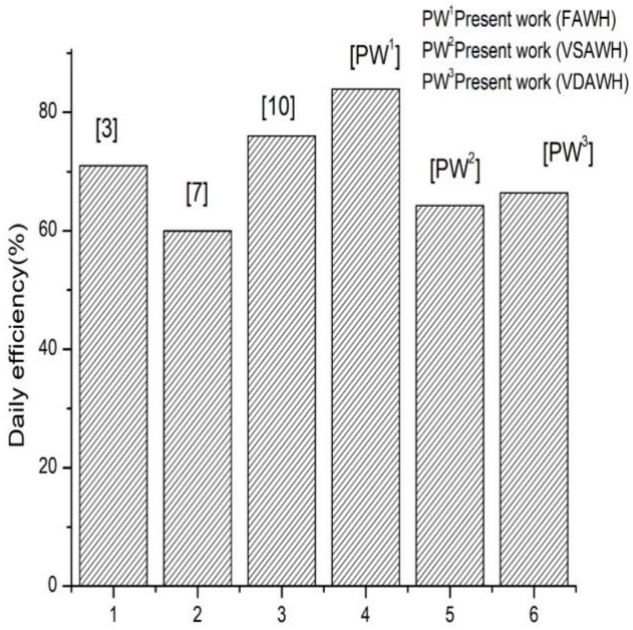

Fig. 17 Comparison of Present Work with Previous Works on Dual-Collector

4. Conclusions

The performance of a V-Corrugated Double-Glazed Dual-purpose Air-Water Heater (V-DAWH) has been investigated. The suggested V-DAWH has a mathematical model that has been created and verified for the weather of Raipur, CG, India. Theoretical research has been done to compare the performance of V-DAWH with V corrugated single glazed air-water heater (V-SAWH), and flat plate air water heater on a typical winter day (F-AWH). The daily efficiency of the proposed air-water heater has been numerically computed and it has been compared with the efficiency of V-SWAH and F-AWH. The effect of the mass stream rate of air flowing in the upper compartment on the performance and efficiency of the proposed heater has been studied numerically.

On a typical day, the degree of heating of air and water is 33.2°C and 55.5°C for V-SWAH and 20.6°C and 41.7°C for F-AWH, respectively. Moreover, in case of V-DAWH is 30°C and 51.4°C, respectively. The maximum air and water temperatures achieved by V-SWAH are 67.2°C and 70.4°C, respectively. The maximum air and water temperatures attained by V-DAWH are 64.2°C and 66.3°C, respectively. According to the findings, the mass stream rate of air flowing in the upper compartment affects the heater's heating performance. The temperature of the outlet air and water drops as the mass stream rate increases.

It is seen that with the increase in mass stream rate the temperature of outlet air and water decreases however the daily efficiency increases. The daily efficiency of V-SAWH is maximum for 0.010kg/s mass stream rate in the upper compartment and it is 83.9% for F-AWH and 66.4% for V-SAWH. The increase in daily efficiency becomes almost constant beyond the mass stream rate of 0.03kg/s.

It is observed that the use of a dual-purpose air-water heater will not only increase the annual usage of the device but can also provide hot air as well as hot water from a single device. When necessary, the device can be used for either air or water heating. The performance can be enhanced further by using a V-corrugated plate, which can provide hot air and water at relatively high temperatures. Although the daily efficiency of F-AWH is maximum, when heated air and water is required at high temperature, the performance of V-SAWH. The proposed design is suitable to meet the demand of hot water as well as air, however for arbitrary demand of hot water the system performance may get affected, In future works the system can be equipped with another insulated tank to accommodate the arbitrary demand of hot water.

References

[1] F. Ayadi, I. Colak, I. Garip, H. Ibrahim. Bulbul, (2020) Impacts of Renewable Energy Resources in Smart Grid. 8th International Conference on Smart Grid (icSmartGrid).(Article).

[2] A. Alkholidi , H. Hamam, (2019). Solar Energy Potentials in Southeastern European Countries : A Case Study. International Journal of SMART GRID,Vol.3, No.2.(Article).

[3] M. Jinwei, S. Wei, J. Jie, Y. Zhang, Z. Aifeng, F. Wen, (2011). Experimental and theoretical study of the efficiency of a dual-function solar collector. Applied Thermal Engineering 31, 1751-1756.(Article)

[4] M.R. Assari, H. B. Tabrizi, I. Jafari, (2011). Experimental and theoretical investigation of dual-purpose solar collector. Solar Energy 85, 601-608.(Article)

[5] O. Nematollahi, P. Alamdari, M. R. Assari, (2014). Experimental investigation of a dual-purpose solar heating system. Energy Conversion and Management 78, 359-366.(Article)

[6] I. Jafari, A. Arshadi, E. Najafpour, N. Hedayat, (2011). Energy and exergy analysis of dual-purpose solar collector., International Journal of Mechanical and Mechotronics Engineering 5(9), 1712-1714. (Article)

[7] V. Shemelin, T. Matuska, (2019). Performance Modelling of Dual Air/Water Collector in Solar Water and Space Heating Application. International Journal of photoenergy. (Article)

[8] A. Venu, A. Palatel, (2013). Simulation studies on porous medium integrated dual-purpose solar collector. International Journal of Renewable Energy Research (IJRER) -3(1).(Article)

[9] N.G. More, R.S. Pole,(2018) Numerical and Experimental Investigation of Dual Purpose Solar Collector, International Journal of Engineering Research & Technology(IJERT)-07-8(Article)

[10] A. J. Qusay, M.J.A. Mahdy, Khuder. H. Ahmed, C. T. Miqdam, (2020). Improve the performance of a solar air heater by adding aluminium chip, paraffin wax and nano SiC. Case Studies (Article)

[11] M. E. Shayan, G. Najafi, F. Ghasemzadeh.(2020) Advance Study of the Parabolic Trough Collector Using Aluminum(III) Oxide, International Journal of SMART GRID, Vol.4,No-3.

[12] V. Msomi, O. Nemraoui, (2017). Improvement of the performance of Solar Water Heater based on Nano Technology.6th International Conference on Renewable Energy Research and Application (ICRERA)(Article)

[13] J. Pukdum, T. Phengpom, K. Sudasna, (2019) Thermal performance of Mixed Asphalt Solar Water Heater. International Journal of Renewable Energy Research (IJRER)(Article)

[14] Y. Choi,(2018). Performance improvement of Liquid type Solar Heat collection system. 7th International Conference on Renewable Energy Research and Application(ICRERA)(Article)

[15] R. Miao, X. Hu, Y. Yu, Y. Zhang, M. Wood, G. Olson (2021). Experimental study of a newly developed dual-purpose solar thermal collector for heat and cold collection. Energy A & B (Article)

[16] M. M. Mkhize, V. Msomi, (2020). Feasibility of a Multistage Solar Still in Southern Africa. 9th International Conference on Renewable Energy Research and Application (ICRERA)(Article)

[17] S.A.A Allah, EI. Gharabawy.(2018). Review on Corrosion in Solar Panels. International Jouurnal of SMART GRID,Vol2,No.4 (Article)

[18] A. Somwanshi, N. Sarkar, (2020). Thermal performance of a dual-purpose collector-cum-storage type air-water heater. Applied Thermal Engineering 171(9), 115094.(Article)

[19] T. A. Yaseen, N. D. Mohklif, M. A. Eleivi, (2019). Performance investigation of an integrated solar water heater with corrugated absorber surface for domestic use., Renewable Energy, doi; 10.1016/J.renene.2019.01.114 (Article)

[20] Md. A. Kareem, M.N.A. Hawalder, (2006). Performance investigation of flat plate V-corrugated and finned air collectors. Energy 31, 452-470. (Article)

[21] AA. El-Sebaii, S. A-Enein, M.R.I. Ramadan, S.M. Shalaby, B.M. Moharram, (2011).Investigation of thermal performance of double pass flat and v-corrugated plate solar air heaters. Energy 36, 1076-1086. (Article)

[22] Md. A. Karim, M.N.A. Hawalder, (2006). Performance evaluation of a v-groove solar air collector for drying applications. Applied Thermal Energy 26, 121-130. (Article)

[23] B.F. Parker, M.R. Lindley, D.G. Colliver, W.E. Murphy, (1993). Thermal performance of three solar air heaters. Solar Energy 51(6), 467-479. (Article)

[24] R. Verma, R. Chandra, H.P. Garg (1991). Parametric studies on the corrugated solar air heaters with and without cover. Renewable Energy 1, 361-371. (Article)

[25] R. Kumar, M. A. Rosen, (2010). Thermal performance of integrated collector storage solar water heater with corrugated absorber surface. Applied Thermal Engineering, 1764-1769. (Article)

[26] F. Channa, R. Bendoud, S. Bounour, C. Hajjaj, A. El-Abidi, H. Ezzaki, A. EI. Rhassouli, R. Rmyali, M. Benhamida, (2018). Design and experimental study of an implemented solar air heater destined for red algae drying. International Journal of Renewable Energy Research (IJRER) -8(4).(Article)

[27] M. H. Basri, Jalaluddin, R. Tarakka, M. Syahid, M. Anis. I. Ramadhani. (2022). Experimental study of modified absorber plate integrated with aluminium foam of solar water heating system. International Journal of Renewable Energy Research. (IJRER)(Article)

[28] G.N. Tiwari, (2002).Solar Energy Fundamentals, Design Modeling and Applications, Narosa publishing house, New Delhi.(Book Chapter)

[29] H. Hottel, B. Woertz, (1942). Performance of flat plate solar heater collectors, Trans. ASME 64, 91-104. (Article)

[30] HS. Heaton, W. Reynolds, W.M. Kays, (1964). Heat transfer in annular passages, simultaneous development of velocity and temperature fields in laminar flow. International Journal Heat Mass Transfer 7, 763-781. (Article)

[31] W.M. Kays, (1980). Convective heat and mass transfer. McGraw Hill, New York.(Book Chapter)

[32] W.H. McAdams, (1954) Heat Transfer. 3rd edition, McGraw Hill, New York.(Book Chapter)

[33] A. Karim, E. Perez, Z. Amin, (2014). Mathematical modelling of counter flow v-groove solar air collectors. Energy 31, 452-470. (Article)

[34] T. Fujii, H. Imura, (1972). Natural convection heat transfer from a plate with arbitrary inclination. International Journal of Heat and Mass Transfer 15 (4), 755-764. (Article)

[35] M.A.S. Malik, F.H. Buelow, (1975). Hydrodynamic and heat transfer characteristics of a heated air duct. Helio technique and Development 2, 3. (Article)

[36] A.E. Kabeel, K. Mecarik (1998). Shape optimization for absorber plates of solar air collectors. Renewable Energy 13, 1361-1378. (Article)

[37] https://weather-and-climate.com/average-monthly-Rainfall-Temperature-Sunshine,raipur-chhattisgarh-in,India , DOA – 25/08/2022

Nomenclature

A_b	Area of base	m^2
A_g	Area of glass covers	m^2
A_p	Absorber plate Area	m^2
b	Half height of groove	m
c_a	Specific heat of air	$Jkg^{-1}K^{-1}$
c_w	Specific heat of water	$Jkg^{-1}K^{-1}$
D_h	Hydraulic diameter	m
D'_h	Approximated hydraulic diameter	m
$H_{\min}$	Minimum height of air Channel	m
h_{cag1}	Convective heat trf between air and upper glass cover	$Wm^{-2}K^{-1}$
h_{cag2}	Convective heat transfer between air and lower glass cover	$Wm^{-2}K^{-1}$
h_{cwb}	Convective heat transfer between ambient and upper glass cover	$Wm^{-2}K^{-1}$
h_{cwb}	Convective heat transfer between water and base	$Wm^{-2}K^{-1}$
h_{ramb}	Radiative heat transfer between ambient and upper glass cover	$Wm^{-2}K^{-1}$
h_{cfg2}	Convective heat transfer between fluid and lower glass cover	$Wm^{-2}K^{-1}$
h_{rg2g1}	Radiative heat transfer between glass covers	$Wm^{-2}K^{-1}$
h_{rpg2}	Radiative heat transfer between absorber plate and lower glass cover	$Wm^{-2}K^{-1}$
I	Total solar radiation	W
K_b	Thermal conductivity of insulation	W/mK
L	Length of collector	m
L_1	Length of absorber plate	m
L_2	Width of collector	m
M_w	Mass of water stored	kg
$\dot{m}_f$	Mass stream rate of fluid in upper compartment	kg/s
T_a	Temperature of air between two glass covers	^oC
T_{amb}	Ambient temp.	^oC
T_g	Temp. of glass cover	^oC
T_{g1}	Temp. of upper glass cover	^oC
T_{g2}	Temp. of lower glass cover	^oC
T_f	Temp. of fluid (air) flowing in upper compartment	^oC
$\bar{T}_f$	Average fluid temperature	^oC
T_p	Temperature of absorber plate	^oC
T_w	Water temperature	^oC
T_b	Temperature of base	^oC
t	Thickness of insulation	m
v_a	Velocity of air flowing over upper glass cover	m/s
v_f	Velocity of fluid (air) flowing in upper compartment	m/s

Greek Letters

α_g	Absorptance of glass cover	
τ_g	Transmittance of glass cover	
α_p	Absorptance of absorber plate	
$\alpha\tau$	Effective transmittance - absorptance product	
ρ_f	Fluid Density (air)	kg/m^3
K_f	Thermal conductivity of fluid (air)	W/mK
μ_f	Dynamic viscosity of fluid (air)	Ns/m^2